

Assessment of the accuracy of interpolation techniques for the mapping of chosen parameters of the soil environment

Urszula Bronowicka-Mielniczuk¹ 

¹ Department of Applied Mathematics and Computer Science, University of Life Sciences in Lublin, ul. Głęboka 28, 20-612 Lublin, Poland
E-mail: urszula.bronowicka@up.lublin.pl

ABSTRACT

The present study addresses the ambiguity of single-metric evaluations by employing a suite of traditional and novel indices combined with principal component and cluster analysis to compare interpolation methods for soil properties. The spatial variability of key soil parameters (pH, organic carbon, total nitrogen, phosphorus, and potassium) was investigated across a study region in two different years, 2015 and 2018. A range of interpolation methods were employed, including ordinary kriging, inverse distance weighting, modified Shepard's method, radial basis functions, empirical Bayesian kriging, triangulation with linear interpolation, nearest neighbour, and natural neighbour. The performance of each method was evaluated using a variety of accuracy measures, including standard metrics such as root mean square error (RMSE) and mean absolute percentage error (MAPE), as well as quantile-based and inequality indices. Principal component analysis (PCA) and cluster analysis (CA) were used to visualise the relationships between interpolation methods and quality measures, thereby facilitating the ranking of methods based on their performance across multiple indices. The analysis yielded distinct clustering patterns among the interpolation methods and quality measures, thus highlighting the strengths and weaknesses of the different techniques. The results indicated that the optimal interpolation method is contingent on the specific soil parameter and the year. Kriging methods, particularly ordinary kriging with various semivariogram models and data transformations, exhibited consistent high performance across different soil parameters.

Keywords: interpolation methods, accuracy measures, principal component analysis, cluster analysis, soil environment.

INTRODUCTION

Accurate mapping of soil parameters is critical for various environmental and agricultural applications, including precision agriculture, land use planning, and ecological risk assessment. Effective soil management relies on detailed and accurate information about the spatial distribution of soil properties (Gołaszewski et al., 2013). This information is essential for optimising fertiliser application, irrigation scheduling and other management practices in precision agriculture (Houlong et al., 2016; Załuski et al., 2022). In environmental assessment, accurate soil maps are critical for understanding the fate and transport of contaminants (Qiao et al., 2018), assessing soil erosion risk (Avalos et al., 2018), and developing effective remediation strategies. Land use

planning also benefits from accurate soil information, as it helps to determine the suitability of land for different uses, such as agriculture, forestry or urban development (Lamsal et al., 2009; Sharma and Sood, 2020). Many studies have highlighted the importance of accurate soil mapping and the challenges associated with achieving it (Buladaco et al., 2024; Igaz et al., 2021). Collectively, these studies highlight the ongoing efforts to improve soil mapping techniques and provide more accurate and readily available soil information for various applications.

With the development of computer techniques and the ability to utilize diverse software, the challenge facing the researcher is the selection of the appropriate interpolation algorithm (Oliver and Webster, 2014). As previous researchers' experiences indicate, there is no universal and uniform

procedure for selecting an interpolation method that would be effective for all types of data (Barrena-González et al., 2022; Bronowicka-Mielniczuk et al., 2019). Therefore, it is necessary to conduct a thorough analysis and evaluation of various interpolation methods to identify the most suitable one for specific applications. This study aims to evaluate the performance of different interpolation methods for mapping selected soil parameters and to provide guidance on the selection of appropriate evaluation techniques based on statistical multivariate analysis.

Traditional methods for evaluating the accuracy of interpolation typically rely on cross-validation procedures and the associated accuracy metrics. It can be asserted with a high degree of confidence that the RMSE is the measure that researchers invariably utilise for this purpose (Fu et al., 2021; Willmott and Matsuura, 2005). Nevertheless, it must be noted that this is not the sole metric employed for this objective. Many authors postulate the use of additional classical metrics, such as the mean error (ME), MSE, MAPE or the coefficient of determination (R^2) between the measured and interpolated values models (Bolivar et al., 2021; Jiang et al., 2022). Lower values of the error statistics indicate higher accuracy of spatial interpolation. However, it is important to note that some researchers argue that these conventional measures may not be sufficient for a comprehensive assessment of the interpolation accuracy (Bronowicka-Mielniczuk and Mielniczuk, 2023; Li and Heap, 2011).

Using only one or two metrics provides a limited and potentially misleading view of a model's performance. Different methods may excel in different ways, and a single metric may not capture the full range of strengths and weaknesses. Certain metrics may inherently favour certain types of interpolation methods. For example, RMSE is sensitive to outliers and may unfairly penalise methods that perform well in most areas but struggle with a few extreme values (Willmott and Matsuura, 2006). This can lead to biased rankings that don't reflect the true suitability of methods for a particular application.

Spatial interpolation is a complex process and the relationships between predicted and observed values can be complicated. Reducing the evaluation to one or two metrics oversimplifies these relationships and can obscure important aspects. A more comprehensive set of metrics allows for a more differentiated comparison and facilitates the selection of a method that best balances various performance criteria (Chai and Draxler, 2014).

This study demonstrates how different interpolation methods perform across a range of evaluation metrics, enabling a more informed selection of the appropriate technique. Some accuracy measures are designed to detect systematic errors like over- or underestimation, whereas traditional metrics like RMSE may not reveal these crucial biases for understanding model behaviour and decision-making implications. Data transformations can also affect the optimal interpolation method and accuracy measure performance. A comprehensive set of measures enables assessing the impact of transformations and selecting the best approach for both interpolation and evaluation. Using a broader set of measures provides a richer basis for comparing interpolation methods, which is important when methods perform similarly on one or two traditional measures, as additional measures can identify subtle differences relevant for specific applications. The principal component analysis and cluster analysis in the study demonstrate this by revealing distinct method clusters based on their multi-metric performance.

DATA AND METHODOLOGY

Study area and data collection

The analysis employed soil data sourced from the LUCAS database, encompassing the most recent data collection campaigns conducted in 2015 (Jones et al., 2020) and 2018 (Fernandez-Ugalde et al., 2022), with the data being provided by the European Soil Data Centre. Comprehensive descriptions of the evaluation process for the soil data within this database are documented in the corresponding reports. The database encompasses the entire European continent and incorporates a range of soil properties, including pH, organic carbon content, and other essential parameters. It is important to note that the soil samples obtained during the two research campaigns were predominantly sourced from the same geographical locations. Moreover, these samples were analysed in a single laboratory, thereby ensuring the high quality and consistency of the data obtained (Fernandez-Ugalde et al., 2022). For the purpose of this study, the results of over 1,290 samples located in Poland were analysed (Fig. 1). The selected soil parameters include soil organic carbon (SOC), total nitrogen (TN), phosphorus (P), extractable potassium (K) and soil pH in H_2O .

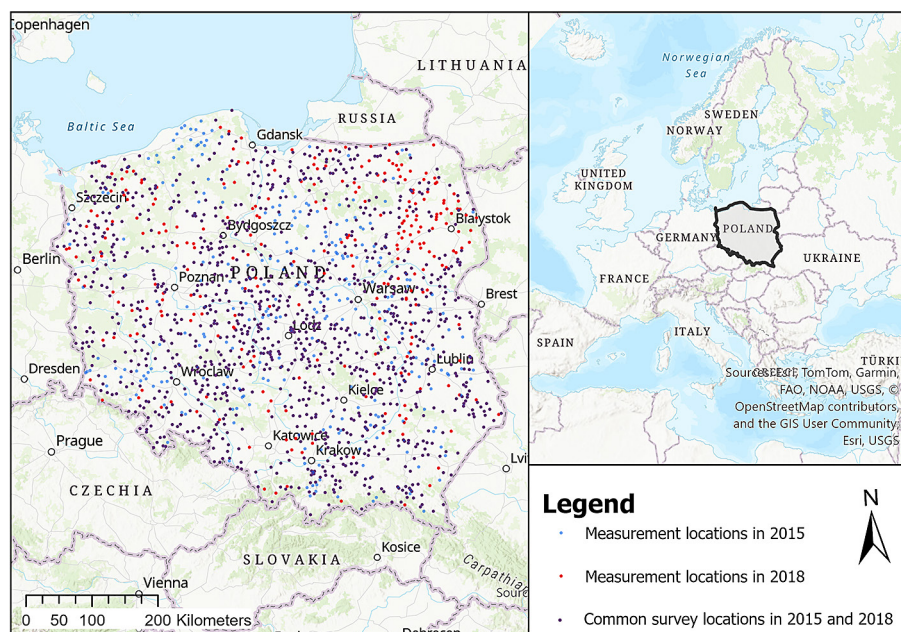


Figure 1. Location of the measurement points

Interpolation methods

The interpolation methods employed in the comparative analysis can be categorised into two broad types: deterministic and geostatistical. The deterministic interpolation techniques estimate values at unsampled locations based on mathematical functions that consider the spatial relationships between the known data points. These functions, which can be distance-based or surface-based, are used to calculate the interpolated values (Webster and Oliver, 2007). The deterministic interpolation techniques employed in the comparative analysis encompassed nearest neighbor (NeN), natural neighbor (NaN), triangulation with linear interpolation (TLI), modified Shepard's method (MS), inverse distance weighting (IDW), and radial basis functions (RBF). In addition, the IDW method incorporated two distinct powers within its formula, relating the distance between points (denoted by p_1 , with an exponent of 1, and p_2 , with an exponent of 2). In contrast, the RBF method utilised disparate basis functions (MQ – multiquadratic, IMQ – inverse multiquadratic, TPS – thin-plate spline, Mlog – multilog, NCS – natural cubic spline) (Rocha, 2009). The geostatistical methods we used were ordinary kriging (OK), applied to both raw and transformed data. Moreover, for the kriging method, various semivariogram models were considered (e.g., cir – circular, gau – Gaussian, exp – exponential, sph – spherical,

sta – stable, JBe – J-Bessel, psph – pentaspherical, hoe – hole effect) to identify the one that provides the best fit to the input data. There was also an investigation into the possibility of a trend in the dataset, but this was not identified. The geostatistical methods were expanded to include the results obtained using empirical Bayesian kriging (EBK). This is a geostatistical interpolation technique that simplifies the complex process of building an accurate kriging model (Esri, 2018). Unlike traditional kriging methods, EBK takes into account the error introduced by the estimation of the underlying semivariogram. The parameters of the semivariogram in EBK are estimated using restricted maximum likelihood (REML), resulting in more accurate predictions (Krivoruchko and Gribov, 2019).

Assessing accuracy

The evaluation of the interpolation techniques was based on a cross-validation method and a set of accuracy indicators calculated from its results. A validation method known as leave-one-out (LOO) was chosen (Webster and Oliver, 2007). In this method, an observation is removed from the data set, and then interpolation is performed to estimate the value of the characteristic under study at the location from which the observation was removed. This process is repeated for all locations associated with the set of existing observations. The resulting estimates are then compared

with the actual observations in order to assess the validity of the interpolation methods. This is achieved by using a selection of error measures. These measures, along with brief descriptions, are summarized in Table 1. Standard metrics such as MAPE and root mean squared error (RMSE) were employed.

In addition, less common but relevant measures, known as the Willmott index and the Waterson index, were also included (see Willmott et al., 2012 for a comprehensive review), as well as measures indicating the inequality of the error distribution (e.g. Gamma, Kolm, Gini statistic). The analysis was further enhanced by incorporating the novel indices detailed in Bronowicka-Mielniczuk and Mielniczuk (2023). These indicators allow the unevenness of errors to be assessed from different perspectives. A significant benefit of the QI and DI indices is its graphical interpretability, which facilitates a more intuitive and nuanced comprehension of results in comparison to purely numerical indices.

Selecting interpolation methods

A multivariate PCA and CA were employed to determine the optimal interpolation method, taking into account a range of accuracy metrics and indicators. This comprehensive approach facilitated the selection of the most appropriate interpolation technique for the given application (Jolliffe and Cadima, 2016). The number of principal components was selected based on the Kaiser criterion, Cattell's scree plot and cumulative percentage of variance explained. Subsequently, a cluster analysis was performed using the k-means method for the grouping of accuracy metrics. For interpolation methods and their variants, the Euclidean metric and Ward's method were utilised. The results of both multivariate analyses were presented in joint biplot graphs. The final stage of the study, following the selection of the optimal interpolation methods for each survey date, entailed the production of maps and their subsequent comparison. In addition to the visual assessment, the technique of comparing the rasters obtained by interpolation was used.

The interpolations and cross-validations were performed in the Surfer (version 28) and ArcGIS Pro (version 3.4.0) software, while the remaining calculations and analysis were conducted in the R computational environment (R Core Team, 2023).

RESULTS AND DISCUSSIONS

The data were collected in two measurement campaigns using 1,377 monitoring stations across Poland. The monitoring sites were located on an irregular grid as shown in Figure 1. The first step in the analysis was to compare the distributions of the analysed soil parameters across the sampling periods.

The distributions of soil parameters in both periods are similar, thus justifying the application of comparative analysis for the maps. The basic descriptive statistics are presented in Table 2. As far as pH is concerned, the only significant change over time to highlight is a decrease in the skewness coefficient. Similarly, both TN and SOC showed negligible changes except for a slight increase in kurtosis and skewness. In contrast, P showed a significant decrease in most of the derived measures with the exception of the coefficient of variation. The trends for K were exactly the opposite of those for P.

The next step in the study was to implement the selected interpolation algorithms. Each of the deterministic interpolations was performed using the same parametric setup over all soil parameters under investigation. For the kriging interpolation, procedures were applied to both the raw and transformed data to eliminate the skewness of the parameters distributions. Logarithmic and/or Box-Cox transformations were applied. Various semivariogram functions were used, with their parameters optimised through algorithms available in the ArcGIS Pro software. The results of the interpolation were utilised to determine the accuracy measures of the interpolation through a leave-one-out cross-validation procedure.

To this end, graphical outputs of multivariate PCA and CA were generated to provide a concise snapshot of the indices under investigation. The results of the two analyses were displayed using joint biplots (Figs. 2–6). Biplots serve as a valuable tool for visualizing the correlations among performance measures, enabling the ranking of interpolation algorithms based on their scores across various indices. Interpolation methods (objects) that are close to each other in the biplot have similar scores on the depicted variables. The angle between variable vectors (representing metrics) indicates their correlation; a small angle shows a strong positive correlation, while perpendicular vectors indicate a weak correlation. Variables with negative correlations are positioned in opposing quadrants of the coordinate

Table 1. Selected measures for the evaluation of interpolation errors

| Measurement | Formula | Comments |
|--|--|--|
| Mean absolute percentage error | $MAPE = \frac{1}{N} \sum_{i=1}^N \left \frac{\zeta_i - z_i}{z_i} \right \cdot 100, \quad z_i > 0$ | Scale-independent measure. A lower value indicates a more accurate prediction. Disadvantages: favours estimates that are lower than the actual values; produces undefined or infinite values for zero or near-zero observed values (Kim and Kim, 2016). |
| Root mean square error | $RMSE = \sqrt{\frac{1}{N} \sum_{i=1}^N (\zeta_i - z_i)^2}$ | Has the same units as observation data. Does not make a distinction between underestimation and overestimation. It gives more weight to large errors and is sensitive to outliers (Kambezidis, 2012). |
| Willmott's index of agreement | $D = 1 - \frac{\sum_{i=1}^N (\zeta_i - z_i)^2}{\sum_{i=1}^N (\zeta_i' + z_i')^2}, \quad z_i' = z_i - \bar{z}, \zeta_i' = \zeta_i - \bar{\zeta}$ | The scale-independent measure ranges from 0 to 1, with 1 representing perfect agreement between the observed and predicted values (Willmott et al., 2012). |
| Watterson's index | $Wsm = \frac{2}{\pi} \sin^{-1} \left\{ 1 - \frac{\sum (\zeta_i - z_i)^2}{s_{\zeta_i}^2 + s_{z_i}^2 + (\bar{\zeta} - \bar{z})^2} \right\}$ | An index originally proposed by Watterson in 1996 for evaluating climate models, non-dimensional (see Willmott et al., 2012 for a comprehensive review). |
| Gamma index | $\gamma = \int_0^{0.5} \gamma(r) \omega(r),$ $\omega(r) = \pi \sin(2\pi r),$ $\gamma(r) = \frac{Q(r) + Q(1-r) - 2Q(0.5)}{Q(1-r) - Q(r)}, \quad 0 < r < 0.5$ | A weighted version of the quantile measure of skewness. A value of 0 indicates that the distribution of the errors obtained is symmetric (Bronowicka-Mielniczuk and Mielniczuk, 2023). |
| Gini coefficient | $G = 1 - 2 \int_0^1 L(\epsilon) d\epsilon$ | The coefficient of Gini was originally developed as a measure of income inequality. However, it is now employed to assess the extent of inequality in various distributions (Cowell, 2011; Pellegrino, 2024). In this study, it serves as an indicator of the deviation of the distribution of errors from an equal distribution, thereby allowing for the estimation of the extent of inequality. The Gini coefficient's theoretical range is from 0 (total equality) to 1 (absolute inequality). There are several ways to compute the Gini coefficient for a dataset. |
| Kolm coefficient | $K = \frac{1}{\kappa} \log \left(\frac{1}{N} \sum_{i=1}^N e^{\kappa(\bar{\epsilon} - \epsilon_i)} \right),$ $\epsilon_i = \frac{ \zeta_i - z_i }{z_i}, \quad i = 1, \dots, N$ | The Kolm inequality index is calculated for a fixed parameter $\kappa > 0$ (Cowell, 2011). In this study, the R ineq package (Zeileis, 2014) was utilised to calculate the index, with a default parameter value of 1 being assumed. |
| fSTM | $fSTM = \iint_{\mathcal{R}^2} I_{[k,r]}(x) \omega(k,r) dk dr,$ $I_{[k,r]} = \sum_{i=1}^N x_i^* \log_{[k,r]}(x),$ $\log_{[k,r]}(x) = x^{r \frac{x^k - x^{-k}}{2k}},$ $\omega(k,r) = 1 - \sqrt{k^2 - r^2}$ | Entropy based inequality measure. A value of zero corresponds to the case of perfect equality between observations and estimates, while a value of one indicates a case of extreme inequality. For a more detailed description, readers are referred to the work of Bronowicka-Mielniczuk and Mielniczuk (2023). |
| Quantile versions of inequality curves (QI1, QI2, QI3) | $QI_{(i)}(\mathbf{x}) = 1 - 2 \int_0^1 L_{(i)}(u, \mathbf{x}) du, \quad i = 1, 2, 3$ $L_{(1)}(u, \mathbf{x}) = u \frac{Q_x(0.5u)}{Q_x(0.5)},$ $L_{(2)}(u, \mathbf{x}) = u \frac{Q_x(0.5u)}{Q_x(1-0.5u)},$ $L_{(3)}(u, \mathbf{x}) = 2u \frac{Q_x(0.5u)}{Q_x(0.5u) + Q_x(1-0.5u)}$ | Quantile versions of inequality curve, are computed for corresponding $L_{(i)}$, where $L_{(1)}$ compares the median of the smallest fraction of the population to the median of the entire population. $L_{(2)}$ gives the ratio between the median of the upper and lower extremes of the population. $L_{(3)}$ provides the median of the lower fraction, relative to the mid-range value of the middle fraction of the population. Graphically interpretable indicator (Bronowicka-Mielniczuk and Mielniczuk, 2023). |
| Directional index (DI1, DI2, DI3, DI4) | $DI_{(i)}(\epsilon) = 2 \int_0^1 u - L_i^*(u, \epsilon) du$ | DI indices which include a modification (L_i^*) for the inequality curve L when the errors have been ranked according to the order of the actual observations. For further details, please refer to Bronowicka-Mielniczuk and Mielniczuk (2023). Graphically interpretable indicator. |

Note: z_i – observed value, s_{z_i} – standard deviations of observed values, $L(\epsilon)$ – Lorenz curve for errors, ζ_i – predicted or estimated value, s_{ζ_i} – standard deviations of predicted values, N – number of observations, $Q_x(u)$ – the sample quantile function, $0 \leq u \leq 1$.

plane. The length of a variable vector along the principal axes reflects its contribution to those axes, with longer vectors having a greater influence on the component. Objects projected orthogonally onto variable vectors can be ranked based on their scores, with projections farthest from the origin in the direction of the vector representing the highest scores. The origin represents the average value for each

variable. It is important to note that the maximum value for both Willmott's and Watterson's indices is one, which indicates a perfect fit.

Principal component analysis was performed on a set of five soil parameters: pH, organic carbon, nitrogen, phosphorus, and potassium, for the years 2015 and 2018. The first three principal components consistently explained a very high

Table 2. Summary statistics describing the distribution of the analysed soil parameters in relation to the survey year

| Soil parameter | Year of survey | Mean | SD | Median | Q ₁ | Q ₃ | Kurtosis | Skewness | V |
|---------------------------|----------------|---------|---------|--------|----------------|----------------|----------|----------|-------|
| pH in H ₂ O | 2015 | 5.500 | 1.028 | 5.37 | 4.67 | 6.22 | 2.330 | 0.452 | 0.187 |
| | 2018 | 5.665 | 1.023 | 5.59 | 4.85 | 6.40 | 2.234 | 0.281 | 0.181 |
| SOC (g kg ⁻¹) | 2015 | 22.434 | 45.437 | 12.10 | 9.00 | 18.80 | 55.789 | 6.813 | 2.025 |
| | 2018 | 22.601 | 46.340 | 12.10 | 9.10 | 18.93 | 60.761 | 7.164 | 2.050 |
| TN (g kg ⁻¹) | 2015 | 2.018 | 3.343 | 1.20 | 1.00 | 1.80 | 55.646 | 6.719 | 1.657 |
| | 2018 | 2.034 | 3.335 | 1.30 | 1.00 | 1.90 | 66.240 | 7.292 | 1.639 |
| P (mg kg ⁻¹) | 2015 | 47.115 | 30.438 | 42.10 | 26.40 | 61.40 | 25.158 | 2.750 | 0.646 |
| | 2018 | 39.489 | 29.325 | 34.10 | 19.80 | 54.33 | 20.468 | 2.523 | 0.743 |
| K (mg kg ⁻¹) | 2015 | 97.331 | 98.066 | 68.80 | 32.00 | 132.40 | 17.923 | 2.802 | 1.008 |
| | 2018 | 109.606 | 102.843 | 82.05 | 45.18 | 144.58 | 64.647 | 5.072 | 0.938 |

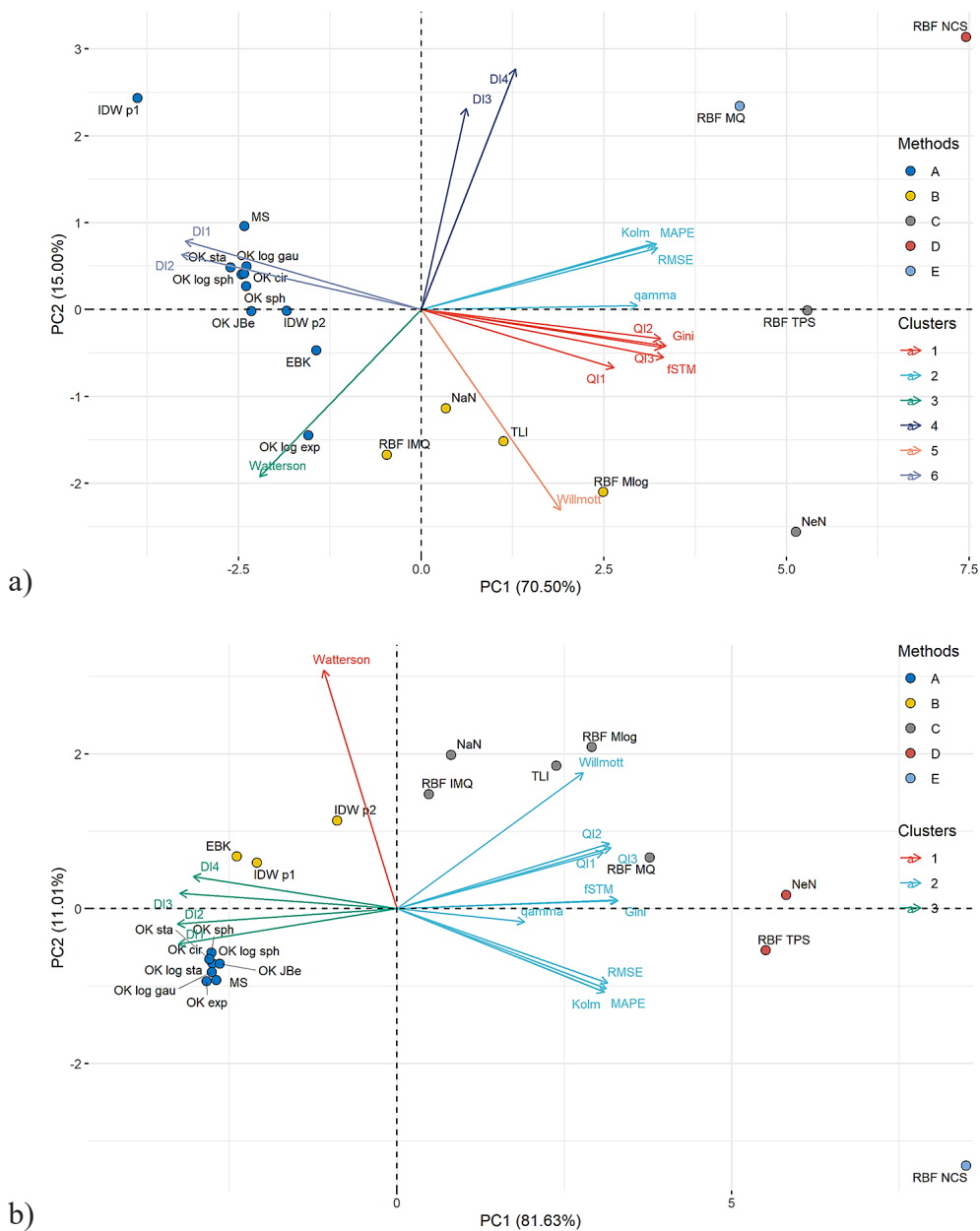


Figure 2. Biplot of principal components for soil pH illustrating the relationships between interpolation methods and quality measures in (a) 2015 and (b) 2018

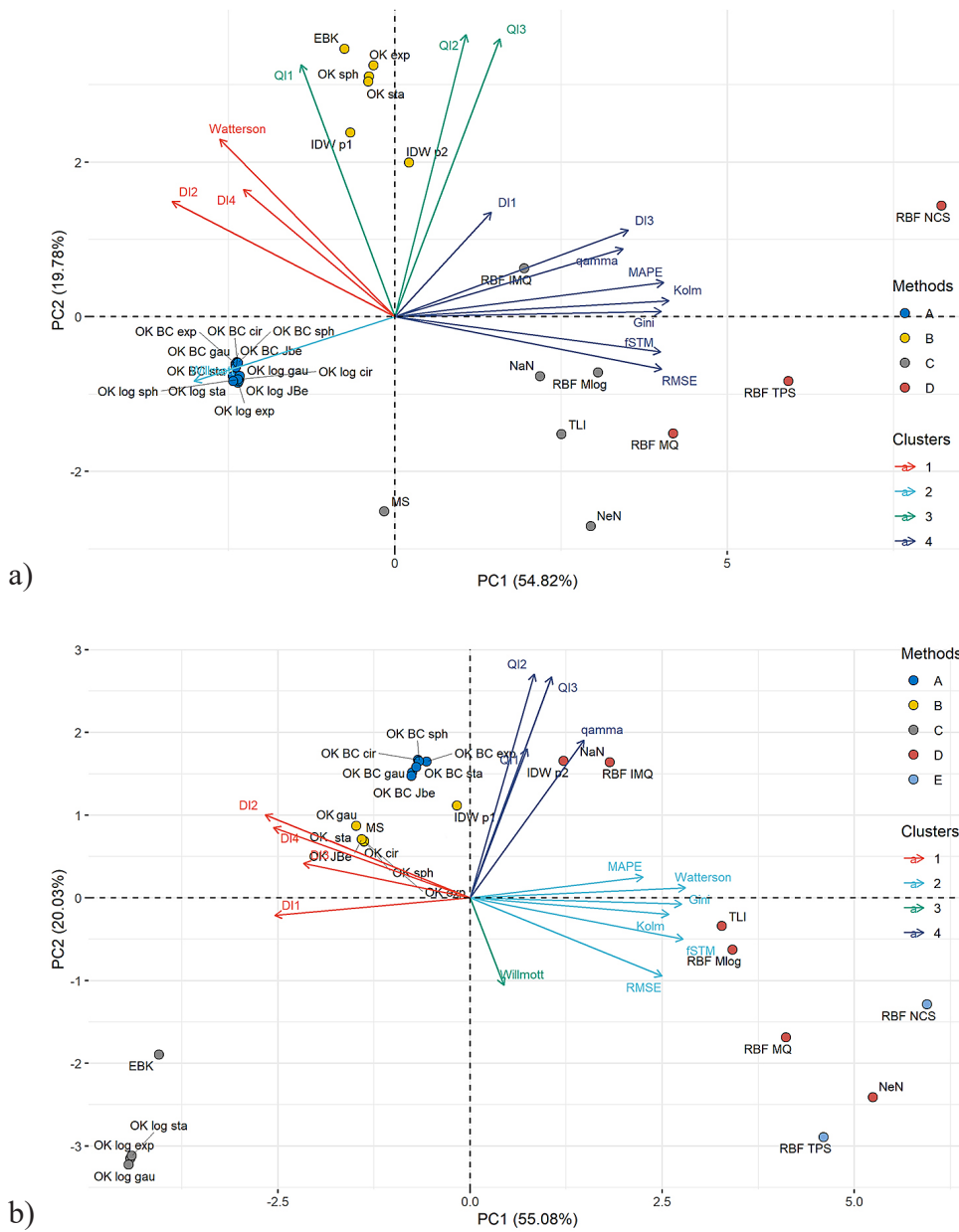


Figure 3. Biplot of principal components for soil organic carbon illustrating the relationships between interpolation methods and quality measures in (a) 2015 and (b) 2018

percentage of the total variance, ranging from 88.1% to 96.2% across all parameters/datasets and both years. This demonstrates that the primary components effectively capture the vast majority of the variability within the data.

While the specific results varied by parameter and year, some general trends emerged. The first principal component (PC1) consistently separated both the standard measures of accuracy (RMSE, MAPE) and Kolm’s statistic from the ensemble of the remaining indices. Although the direction of the correlation varied, there was a significant association with PC1 across the board. PC2 and PC3

typically captured variability in other indices, such as Willmott, Watterson, and quantile measures (Q indices). Strong correlations were observed within the variants of both the D and Q indices, indicating an association between the corresponding criteria of model quality. This was particularly evident for the D indices, which often formed tight clusters.

The biplots (Figs. 2–6) visually represent the distinct clusters formed by both the interpolation methods and the quality measures used in the analysis. While the specific cluster arrangements varied between parameters and years, the kriging methods (with and without data transformation) frequently

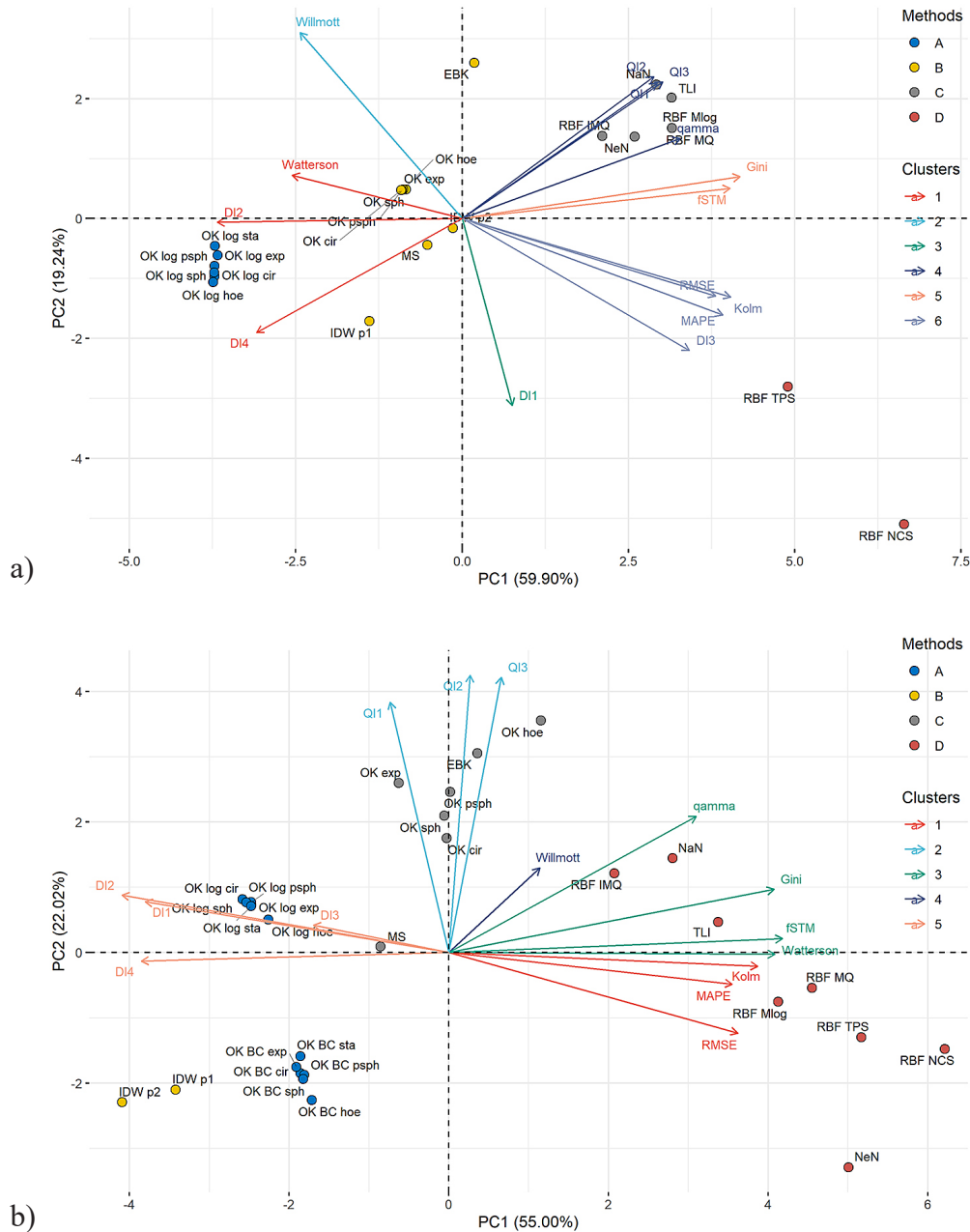


Figure 4. Biplot of principal components for total nitrogen illustrating the relationships between interpolation methods and quality measures in (a) 2015 and (b) 2018

clustered together, as did IDW, MS, and sometimes EBK. The remaining deterministic methods typically formed separate, smaller clusters.

While some quality measures evidently distinguished between different types of interpolation methods (e.g., kriging vs. deterministic), they were often less effective in discriminating among methods within the same type. For instance, different variants of kriging often clustered closely together, even when applied with different data transformations. This suggests that relying solely on these indices may not be sufficient for selecting the best method within a given category.

The extensive principal component and cluster analysis enabled the identification of interpolation techniques that most effectively capture the spatial patterns of soil properties across the study region over the two time periods.

For pH, ordinary kriging with the J-Bessel model was recommended in the first term (Fig. 2a) of the study and EBK in the following term (Fig. 2b).

With respect to SOC, ordinary kriging with a stable model performed well on Box-Cox transformed data in 2015 (Fig. 3a), and ordinary kriging without transformation and Gaussian model in 2018 (Fig. 3b).

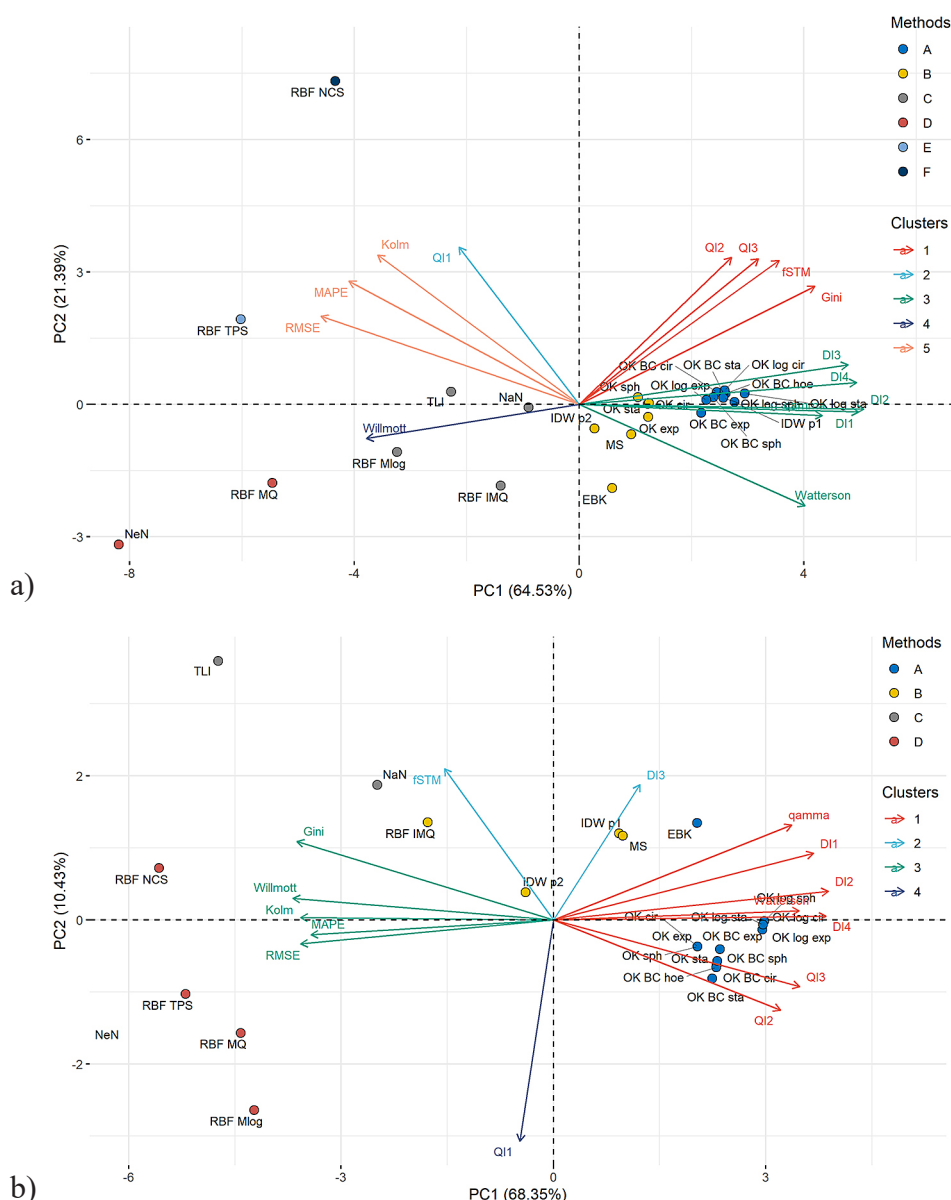


Figure 5. Biplot of principal components for phosphorus illustrating the relationships between interpolation methods and quality measures in (a) 2015 and (b) 2018

The optimal methods for TN were determined to be ordinary kriging with stable and circular models, respectively, for log-transformed data from 2015 (Fig. 4a) and 2018 (Fig. 4a).

For P, ordinary kriging with an exponential semivariogram, based on Box-Cox transformed data from 2015 (Fig. 5a), was identified as the most appropriate approach, while for 2018, the most suitable method was determined to be ordinary kriging with a spherical model, based on a logarithmic transformation (Fig. 5b).

In contrast, ordinary kriging with a circular model for the raw data in 2015 (Fig. 6a) and ordinary kriging with a Gaussian model in 2018 (Fig. 6b), together with logarithmically transformed

data, were identified as the most effective approaches for K.

Table 3 presents the results of the selection of interpolation algorithms based on the PCA analysis and Figures 2–6. In addition, the methods with the lowest RMSE and MAPE values are summarised.

In particular, the same result based on ranking for RMSE was obtained in only one case, for K in 2018. The ranking performed on the basis of the MAPE metric, however, shows overlap in three of all ten cases analysed (P and SOC for 2015 and pH for 2018). In the remaining cases, the two techniques indicate different models. It is also noteworthy that, in the ranking for RMSE, half of the selected models belong to deterministic

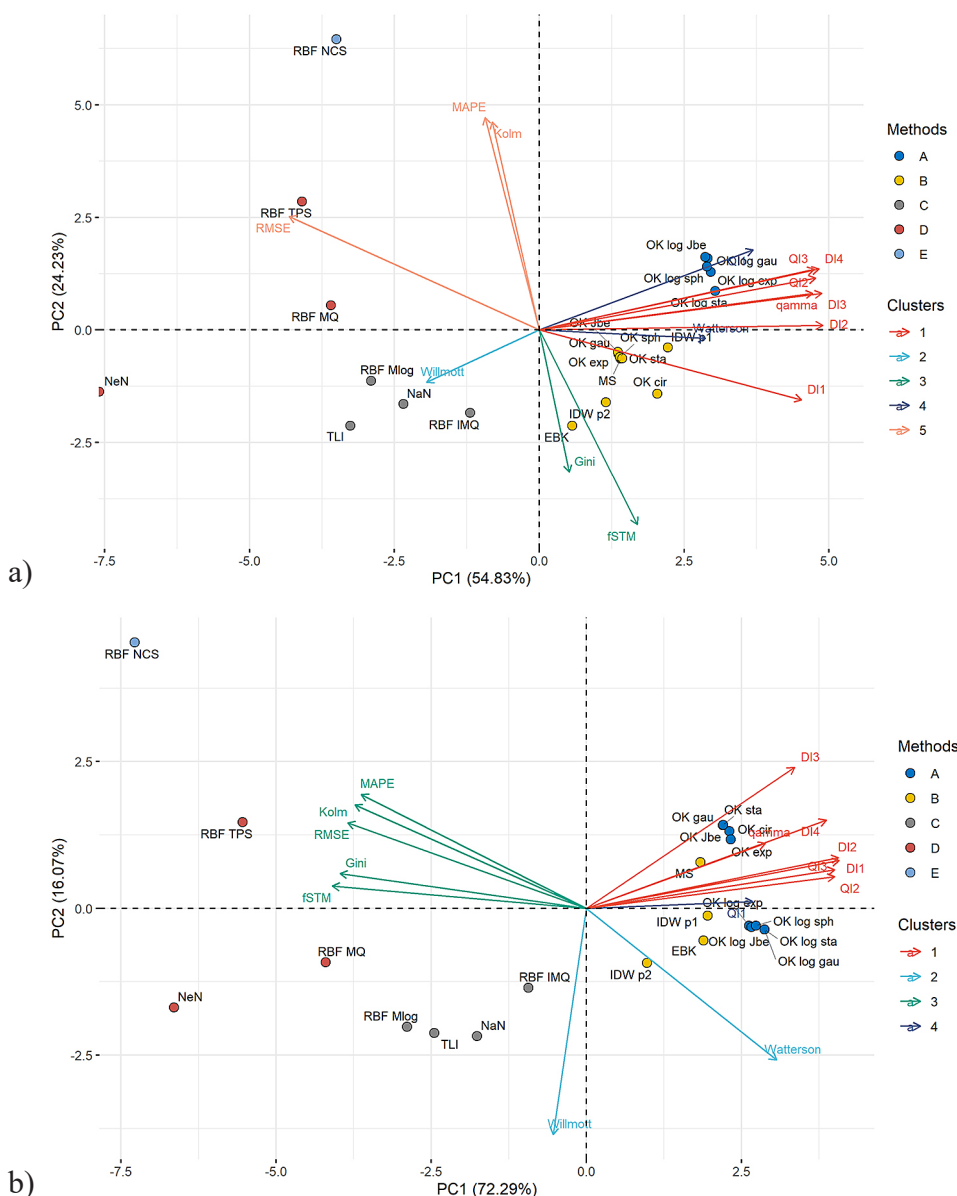


Figure 6. Biplot of principal components for potassium illustrating the relationships between interpolation methods and quality measures in (a) 2015 and (b) 2018

Table 3. Selection of optimal interpolation methods using single metric ranking and multimetric with PCA

| Soil parameter | Year of survey | Single metric ranking | | Multimetric with PCA |
|---------------------------|----------------|-----------------------|-------------|----------------------|
| | | RMSE | MAPE | |
| pH in H ₂ O | 2015 | OK sta | OK sta | OK JBe |
| | 2018 | OK exp | EBK | EBK |
| SOC (g kg ⁻¹) | 2015 | MS | OK log sta | OK log sta |
| | 2018 | EBK | OK log sta | OK gau |
| TN (g kg ⁻¹) | 2015 | IDW p1 | OK log sta | OK sta |
| | 2018 | IDW p1 | OK log psph | OK log sph |
| P (mg kg ⁻¹) | 2015 | IDW p1 | OK BC exp | OK BC exp |
| | 2018 | OK BC hoe | OK BC cir | OK log sph |
| K (mg kg ⁻¹) | 2015 | IDW p1 | RBF IMQ | OK log cir |
| | 2018 | OK log gau | OK log exp | OK log gau |

Note: Bold indicates the method identified as optimal by both selection methods.

methods, and in most of the ten cases, the method selected based on the ranking does not belong to the same cluster.

The results obtained in this study following method selection were utilised to create maps of the distribution of soil parameters in the area under consideration in 2015 and 2018. Moreover, the comparative analysis was supplemented by

a map indicating the changes (decrease or increase) in the concentration of the parameter over the established study periods. (Figs. 7–11). However, it should be emphasised that the main objective of the study was to propose a different way of evaluating the interpolation and its selection. Identifying the potential causes of the changes that have occurred, or assessing the

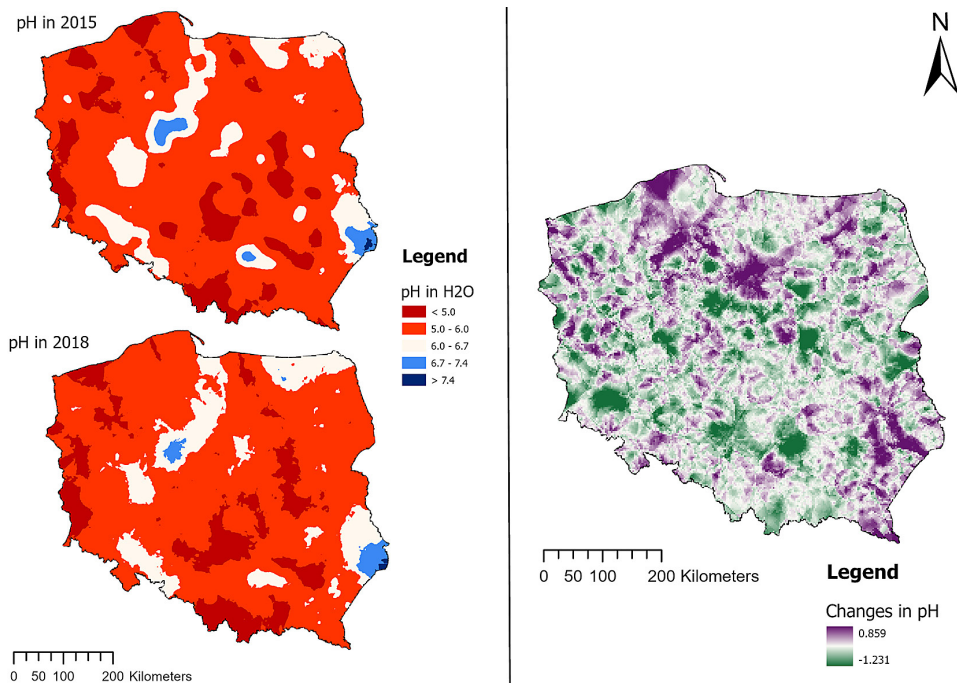


Figure 7. Comparison of interpolation results for soil pH

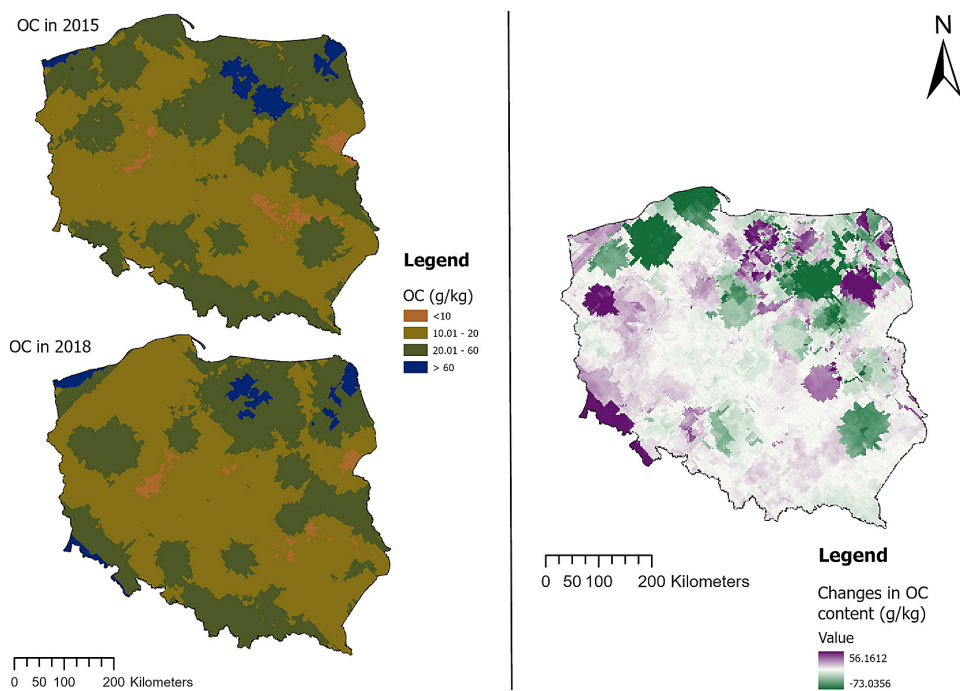


Figure 8. Comparison of interpolation results for organic carbon content

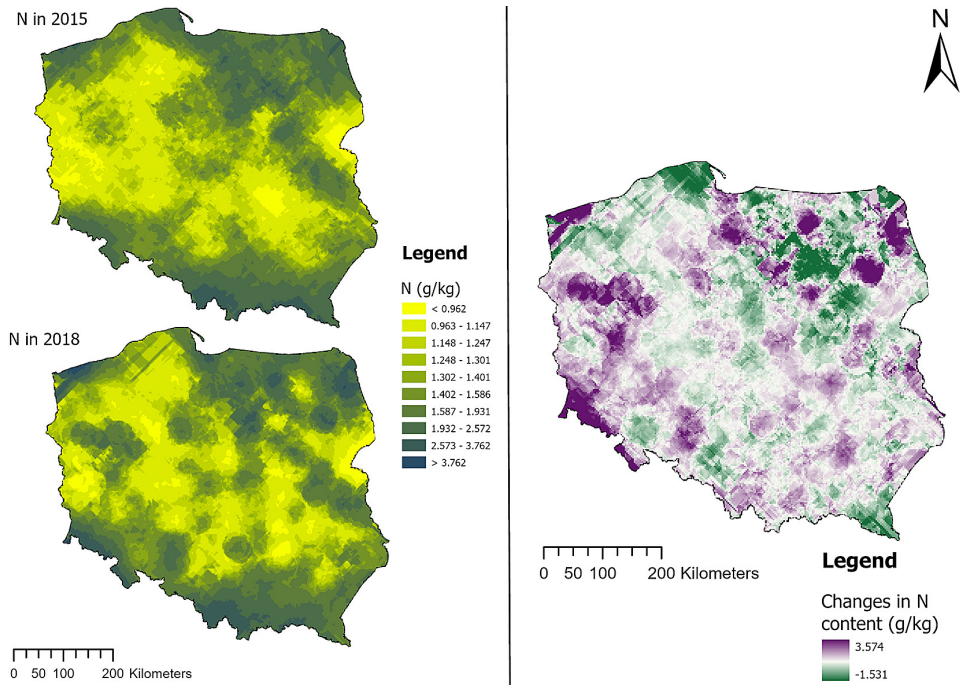


Figure 9. Comparison of interpolation results for total nitrogen content

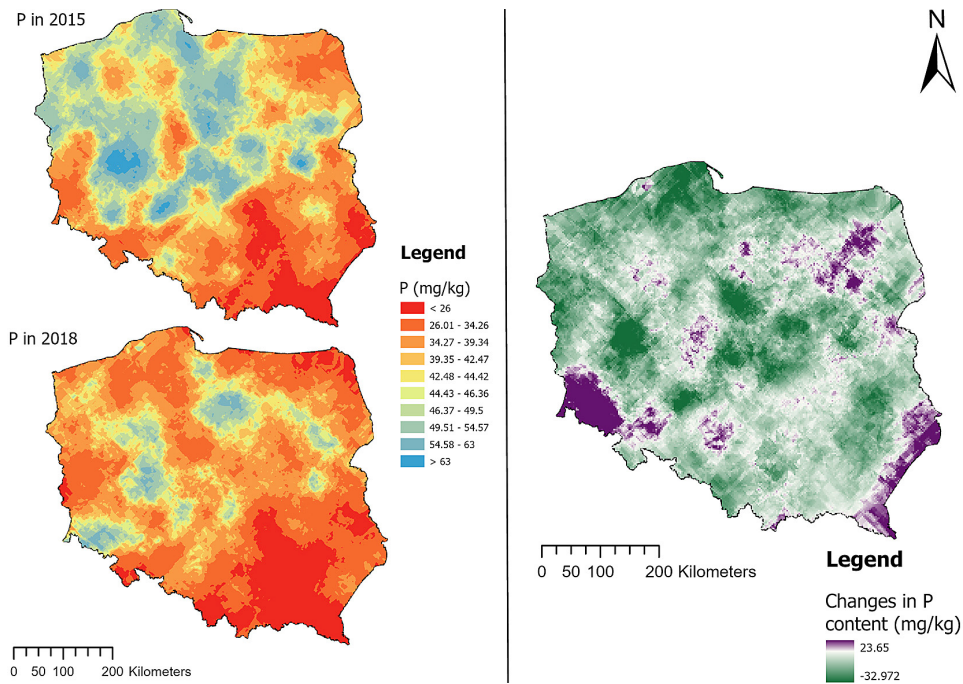


Figure 10. Comparison of interpolation results for phosphorus content

condition of the soil, requires the consideration of other factors that are beyond the purpose and scope of this work.

Poland is characterised by a very high proportion of acidic and very acidic soils (Fig. 7). Soil acidification in Poland is the result of a combination of natural and human factors (Ochal et al., 2017). The local climate and the type of bedrock are key

elements in this regard. It is noteworthy that over 90% of Polish soils originate from acidic rocks deposited as a result of glacial processes. It should be underlined that the distribution of this soil parameter remained quite stable over the period considered (Fig. 7). This indicates on the dominant role of soil and climatic conditions in shaping soil pH levels in Poland. Generally, a decrease in pH by 1.2

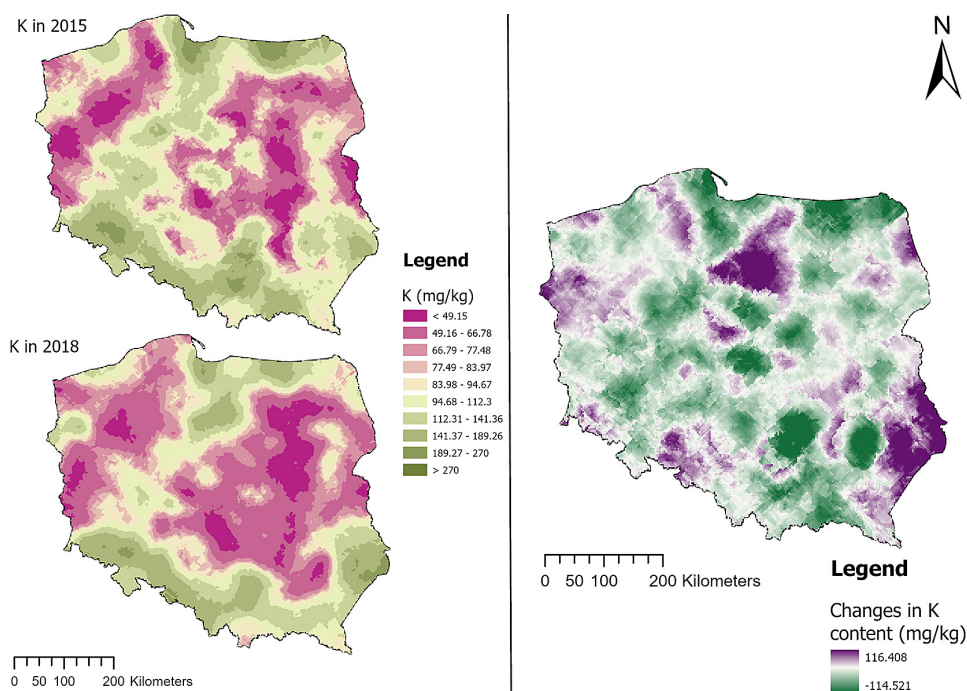


Figure 11. Comparison of interpolation results for potassium content

or an increase by 0.8 resulted in the change of soil reaction class to a small extent (Fig. 7).

In most parts of Poland, soils with low and very low SOC contents, i.e. below 20 g/kg, are predominant. The greatest variations in SOC levels were observed mainly in northern and central-eastern parts of Poland (Fig. 8). According to some authors (Kuśmierz et al., 2023; Zimnoch et al., 2024), clay-rich soils, $\text{pH} > 5.5$, water content as well as mineral and organic fertilization, crop rotations, minimum tillage, intercropping, and management of crop residue are the factors significantly influencing the accumulation of soil organic carbon. An elevation in SOC levels was observed in most of the country (Fig. 8) between 2015 and 2018. Siebielec et al. (2020) also noticed increases in organic carbon content in Polish soils with an initial value of this parameter below 15 g/kg.

Since over 90% of TN occurs in organic forms in the surface layer of most soils, changes in its contents between 2015 and 2018 followed a similar pattern to the alteration in SOC levels (Fig. 9 and Fig. 8). As highlighted by Fu et al. (2021) and Xue et al. (2013), variations in total nitrogen concentrations can be attributed to different factors. Key among these are land use, crop rotation, landscape position, climatic conditions, and fertilisation practices.

Phosphorus and potassium were the parameters for which the most significant fluctuations

were observed over time, with a marked downward trend in the content of these elements in the soil (Fig. 10). In the case of phosphorus, an increase in the content of this parameter was observed only in two compact areas, located in the south-eastern and western parts of Poland. Conversely, the most substantial decreases in potassium content were noted in the central and central-eastern Poland areas (Fig. 11). The phosphorus accumulation and its loss from soils are complex and depend on many factors. Some of the most important are fertilization, crop rotation, changes in land use, pH , and the content of organic matter, iron, and aluminum in the soils (Grosso et al., 2015). Bashir et al. (2024) indicated the relationship between potassium content and soil properties such as organic carbon, clay content, plant species, and topography. It should be noted that in Poland for many years there has been an unfavourable N:P:K ratio in the mineral fertilizers used, to the detriment of phosphorus and potassium.

CONCLUSIONS

This study demonstrated the effectiveness of principal component analysis for evaluating and comparing the performance of various spatial interpolation methods for soil parameters. The ranking and comprehensive approaches combined

with PCA analysis were compared, and the results of these techniques rarely overlap. Furthermore, the analysis revealed distinct relationships between different types of accuracy measures. PC1 often differentiated standard accuracy measures from inequality and asymmetry indices. The relative importance of different quality measures varied depending on the specific soil parameter and year, suggesting that the choice of relevant quality measures should be context-specific. Finally, deterministic methods beyond kriging, IDW, MS, and EBK often exhibited unique performance characteristics, indicating their potential value in specific applications.

Beyond soil property mapping, the results of this study have broader implications for environmental monitoring and pollution assessment. The refined selection of interpolation methods can improve predictions of soil conditions and the modelling of contaminant migration, ultimately supporting more effective environmental management and remediation strategies.

REFERENCES

1. Avalos, F. A. P., Silva, M. L. N., Batista, P. V. G., Pontes, L. M., & de Oliveira, M. S. (2018). Digital soil erodibility mapping by soilscape trending and kriging. *Land Degradation and Development*, 29(9), 3021–3028. <https://doi.org/10.1002/LDR.3057>
2. Barrera-González, J., Lavado Contador, J. F., & Pulido Fernández, M. (2022). Mapping soil properties at a regional scale: Assessing deterministic vs. geostatistical interpolation methods at different soil depths. *Sustainability*, 14(16), 10049. <https://doi.org/10.3390/su141610049>
3. Bashir, O., Bangroo, S. A., Shafai, S. S., Senesi, N., Naikoo, N. B., Kader, S., & Jaufer, L. (2024). Unlocking the potential of soil potassium: Geostatistical approaches for understanding spatial variations in Northwestern Himalayas. *Ecological Informatics*, 81, 102592. <https://doi.org/10.1016/J.ECOINF.2024.102592>
4. Bolivar, A., Camacho, C., Ordonez, N., Gutierrez, J., Alvarez, G., Guevara, M., Olivera, C., Federico Olmedo, G., Bunning, S., & Vargas, R. (2021). Estimation of soil organic carbon in Colombia, a territory management tool. *ECOSISTEMAS*, 30(1). <https://doi.org/10.7818/ECOS.2019>
5. Bronowicka-Mielniczuk, U., & Mielniczuk, J. (2023). New indices to quantify patterns of relative errors produced by spatial interpolation models – A comparative study by modelling soil properties. *Ecological Indicators*, 154, 110551. <https://doi.org/https://doi.org/10.1016/j.ecolind.2023.110551>
6. Bronowicka-Mielniczuk, U., Mielniczuk, J., Obroślak, R., & Przystupa, W. (2019). A comparison of some interpolation techniques for determining spatial distribution of nitrogen compounds in groundwater. *International Journal of Environmental Research*, 13(4), 679–687. <https://doi.org/10.1007/s41742-019-00208-6>
7. Buladaco, M. S. I., Tandugon, H. M. F., Bunquin, M. A. B., Sanchez, P. B., Bugia, S. A. C., Yales, N. A. P., & Casacop, S. M. (2024). Mapping and assessment of within-field spatial variability of soil pH, electrical conductivity, and particle size distribution to delineate management zones. *Ecological Engineering & Environmental Technology*, 25(10), 75–86. <https://doi.org/10.12912/27197050/191244>
8. Chai, T., & Draxler, R. R. (2014). Root mean square error (RMSE) or mean absolute error (MAE)? -Arguments against avoiding RMSE in the literature. *Geoscientific Model Development*, 7(3), 1247–1250. <https://doi.org/10.5194/GMD-7-1247-2014>
9. Cowell, F. (2011). *Measuring Inequality* (3rd ed.). Oxford University Press. <https://doi.org/10.1093/acprof:osobl/9780199594030.001.0001>
10. Dreshaj, A., Orqusha, N., Berljajli, V., & Osmanaj, A. (2024). Quality assessment through land use change, land surface temperature - an environmental factors analysis. *Ecological Engineering & Environmental Technology*, 25(6), 200–207. <https://doi.org/10.12912/27197050/187041>
11. Elbasiouny, H., Abowaly, M., Abu-Alkheir, A., & Gad, A. A. (2014). Spatial variation of soil carbon and nitrogen pools by using ordinary Kriging method in an area of north Nile Delta, Egypt. *CATENA*, 113, 70–78. <https://doi.org/10.1016/J.CATENA.2013.09.008>
12. Esri. (2018). *ArcGIS* (10.6.1). Esri. <https://www.esri.com>
13. Fernandez-Ugalde, O., Scarpa, S., Orgiazzi, A., Panagos, P., Marc, V. L., Marechal, A., & Jones, A. (2022). *LUCAS 2018 Soil Module*. Publications Office of the European Union. <https://doi.org/10.2760/215013>
14. Fu, T., Gao, H., & Liu, J. (2021). Comparison of different interpolation methods for prediction of soil salinity in arid irrigation region in Northern China. *Agronomy*, 11(8). <https://doi.org/10.3390/agronomy11081535>
15. Göç, C., Bulut, S., & Bolat, F. (2017). Comparison of different interpolation methods for spatial distribution of soil organic carbon and some soil properties in the Black Sea backward region of Turkey. *Journal of African Earth Sciences*, 134, 85–91. <https://doi.org/10.1016/j.jafrearsci.2017.06.014>
16. Gołaszewski, J., Załuski, D., Żuk-Gołaszewska, K., & Grzela, K. (2013). Geostatistical methods as

- auxiliary tools in field plot experimentation. In Stafford J.V. (Ed.), *Precision agriculture '13* (pp. 499–506). Wageningen Academic Publishers. https://doi.org/10.3920/978-90-8686-778-3_61
17. Gong, G., Mattevada, S., & O'Bryant, S. E. (2014). Comparison of the accuracy of kriging and IDW interpolations in estimating groundwater arsenic concentrations in Texas. *Environmental Research*, 130, 59–69. <https://doi.org/10.1016/j.envres.2013.12.005>
18. Groppo, J. D., Lins, S. R. M., Camargo, P. B., Assad, E. D., Pinto, H. S., Martins, S. C., Salgado, P. R., Evangelista, B., Vasconcellos, E., Sano, E. E., Pavão, E., Luna, R., & Martinelli, L. A. (2015). Changes in soil carbon, nitrogen, and phosphorus due to land-use changes in Brazil. *Biogeosciences*, 12(15), 4765–4780. <https://doi.org/10.5194/BG-12-4765-2015>
19. Houlong, J., Daibin, W., Chen, X., Shuduan, L., Hongfeng, W., Chao, Y., Najia, L., Yiyin, C., & Lina, G. (2016). Comparison of kriging interpolation precision between grid sampling scheme and simple random sampling scheme for precision agriculture. *Eurasian J Soil Sci*, 5(1), 62–73. <https://doi.org/10.18393/ejss.2016.1.062-073>
20. Igaz, D., Šinka, K., Varga, P., Vrbičanová, G., Aydın, E., & Tárnik, A. (2021). The evaluation of the accuracy of interpolation methods in crafting maps of physical and hydro-physical soil properties. *Water* 2021, Vol. 13, Page 212, 13(2), 212. <https://doi.org/10.3390/W13020212>
21. Jiang, B., Xu, W., Zhang, D., Nie, F., & Sun, Q. (2022). Contrasting multiple deterministic interpolation responses to different spatial scale in prediction soil organic carbon: A case study in Mollisols regions. *Ecological Indicators*, 134, 108472. <https://doi.org/10.1016/J.ECOLIND.2021.108472>
22. John, K., Afu, S. M., Isong, I. A., Aki, E. E., Kebonye, N. M., Ayito, E. O., Chapman, P. A., Eyong, M. O., & Penížek, V. (2021). Mapping soil properties with soil-environmental covariates using geostatistics and multivariate statistics. *International Journal of Environmental Science and Technology*, 18(11), 3327–3342. <https://doi.org/10.1007/s13762-020-03089-x>
23. Jolliffe, I. T., & Cadima, J. (2016). Principal component analysis: a review and recent developments. *Philosophical Transactions of the Royal Society A: Mathematical, Physical and Engineering Sciences*, 374(2065), 20150202. <https://doi.org/10.1098/rsta.2015.0202>
24. Jones, A., Fernandez-Ugalde, O., & Scarpa, S. (2020). *LUCAS 2015 Topsoil Survey. Presentation of dataset and results*. <https://doi.org/10.2760/616084>
25. Kambezidis, H. D. (2012). The Solar Resource. *Comprehensive Renewable Energy*, 27–84. <https://doi.org/10.1016/B978-0-08-087872-0.00302-4>
26. Kim, S., & Kim, H. (2016). A new metric of absolute percentage error for intermittent demand forecasts. *International Journal of Forecasting*, 32(3), 669–679. <https://doi.org/10.1016/j.ijforecast.2015.12.003>
27. Krivoruchko, K., & Gribov, A. (2019). Evaluation of empirical Bayesian kriging. *Spatial Statistics*, 32, 100368. <https://doi.org/10.1016/J.SPASTA.2019.100368>
28. Kuśmierz, S., Skowrońska, M., Tkaczyk, P., Lipiński, W., & Mielniczuk, J. (2023). Soil organic carbon and mineral nitrogen contents in soils as affected by their pH, texture and fertilization. *Agronomy* 2023, 13(1), 267. <https://doi.org/10.3390/AGRONOMY13010267>
29. Lamsal, S., Bliss, C. M., & Graetz, D. A. (2009). Geospatial mapping of soil nitrate-nitrogen distribution under a mixed-land use system. *Pedosphere*, 19(4), 434–445. [https://doi.org/10.1016/S1002-0160\(09\)60136-3](https://doi.org/10.1016/S1002-0160(09)60136-3)
30. Li, J., & Heap, A. D. (2011). A review of comparative studies of spatial interpolation methods in environmental sciences: Performance and impact factors. *Ecological Informatics*, 6(3–4), 228–241. <https://doi.org/10.1016/J.ECOINF.2010.12.003>
31. Liu, X., Hu, J., & Ma, J. (2011). Quantitative Evaluation of Spatial Interpolation Models Based on a Data-Independent Method. In D. Chen (Ed.), *Advances in Data, Methods, Models and Their Applications in Geoscience*. IntechOpen. <https://doi.org/10.5772/28365>
32. Ochal, P., Jadczyzyn, T., Matyka, M., Madej, A., Rutkowska, A., Smreczak, B., & Łysiak, M. (2017). *Środowiskowe aspekty zakwaszenia gleb w Polsce (In Polish). Environmental aspects of soil acidification in Poland*. 43. Institute of Soil Science and Plant Cultivation State Research Institute: Puławy. https://www.izbarolnicza.lodz.pl/sites/default/files/IUNG_ekspertyza_wapnowanie_17.10.2017r.pdf
33. Oliver, M., & Webster, R. (2014). A tutorial guide to geostatistics: Computing and modelling variograms and kriging. *Catena*, 113, 56–69. <https://doi.org/10.1016/J.CATENA.2013.09.006>
34. Omićević, D., Krdžalić, D., & Vrce, E. (2023). Comparison of Methods of Prediction of Heavy Metals in the Soil Using R. *Lecture Notes in Networks and Systems*, 539 LNNS, 664–673. https://doi.org/10.1007/978-3-031-17697-5_50
35. Pellegrino, S. (2024). *The Gini coefficient: its origins* (No.70-Version No. 2). <https://www.bemservizi.unito.it/repec/tur/wpapnw/m86.pdf>
36. Qiao, P., Lei, M., Yang, S., Yang, J., Guo, G., & Zhou, X. (2018). Comparing ordinary kriging and inverse distance weighting for soil as pollution in Beijing. *Environmental Science and*

- Pollution Research*, 25, 15597–15608. <https://doi.org/10.1007/s11356-018-1552-y>
37. R Core Team. (2023). *R: A language and environment for statistical computing*. R Foundation for Statistical Computing. <https://www.r-project.org>
38. Rocha, H. (2009). On the selection of the most adequate radial basis function. *Applied Mathematical Modelling*, 33, 1573–1583.
39. Sharma, R., & Sood, K. (2020). Characterization of spatial variability of soil parameters in apple orchards of Himalayan region using geostatistical analysis. *Communications in Soil Science and Plant Analysis*, 51(8), 1065–1077. <https://doi.org/10.1080/00103624.2020.1744637>
40. Siebielec, G., Łopatka, A., Smreczak, B., Kaczyński, R., Siebielec, S., Koza, P., & Dach, J. (2020). Materia organiczna w glebach mineralnych Polski (In Polish). Organic matter in mineral soils of Poland. *Studia i Raporty IUNG-PIB*, 68(18), 9–30. <https://doi.org/10.26114/sir.iung.2020.64.01>
41. Webster, R., & Oliver, M. (2007). *Geostatistics for Environmental Scientists* (2nd ed.). John Wiley & Sons Ltd. <https://www.wiley.com/en-us/Geostatistics+for+Environmental+Scientists%2C+2nd+Edition-p-9780470028582>
42. Willmott, C. J., & Matsuura, K. (2005). Advantages of the mean absolute error (MAE) over the root mean square error (RMSE) in assessing average model performance. *Climate Research*, 30(1), 79–82. <https://doi.org/10.3354/CR030079>
43. Willmott, C. J., & Matsuura, K. (2006). On the use of dimensioned measures of error to evaluate the performance of spatial interpolators. *International Journal of Geographical Information Science*, 20(1), 89–102. <https://doi.org/10.1080/13658810500286976>
44. Willmott, C. J., Robeson, S. M., & Matsuura, K. (2012). A refined index of model performance. *International Journal of Climatology*, 32(13), 2088–2094. <https://doi.org/10.1002/joc.2419>
45. Xue, Z., Cheng, M., & An, S. (2013). Soil nitrogen distributions for different land uses and landscape positions in a small watershed on Loess Plateau, China. *Ecological Engineering*, 60, 204–213. <https://doi.org/10.1016/J.ECOLENG.2013.07.045>
46. Załuski, D., Bronowicka-Mielniczuk, U., Mielniczuk, J., Krzyżaniak, M., & Stolarski, M. J. (2022). Control of soil variability in data analysis from camelina and crambe field breeding experiments with check plots. *Archives of Agronomy and Soil Science*, 1–11. <https://doi.org/10.1080/03650340.2022.2152010>
47. Zeileis, A. (2014). *ineq: Measuring Inequality, Concentration, and Poverty*. R package version 0.2-13. <https://cran.r-project.org/package=ineq>
48. Zimnoch, U., Bogusz, P., Brodowska, M., & Michalak, J. (2024). The trend of changes in soil organic carbon content in Poland over recent years. *Archives of Environmental Protection*, 50(1), 35–44. <https://doi.org/10.24425/aep.2024.149430>